

# Mechanisms Underlying Stabilization of Temporally Summated Muscle Contractions in the Lobster (*Panulirus*) Pyloric System

LEE G. MORRIS<sup>1</sup> AND SCOTT L. HOOPER<sup>2</sup>

<sup>1</sup>Department of Biology, Emory University, Atlanta, Georgia 30322; and <sup>2</sup>Neuroscience Program, Department of Biological Sciences, Ohio University, Athens, Ohio 45701

Received 20 April 2000; accepted in final form 20 September 2000

**Morris, Lee G. and Scott L. Hooper.** Mechanisms underlying stabilization of temporally summated muscle contractions in the lobster (*Panulirus*) pyloric system. *J Neurophysiol* 85: 254–268, 2001. Muscles are the final effectors of behavior. The neural basis of behavior therefore cannot be completely understood without a description of the transfer function between neural output and muscle contraction. To this end, we have been studying muscle contraction in the well-investigated lobster pyloric system. We report here the mechanisms underlying stabilization of temporally summating contractions of the very slow dorsal dilator muscle in response to motor nerve stimulation with trains of rhythmic shock bursts at a physiological intraburst spike frequency (60 Hz), physiological cycle periods (0.5–2 s), and duty cycles from 0.1 to 0.8. For temporal summation to stabilize, the rise and relaxation amplitudes of the phasic contractions each burst induces must equalize as the rhythmic train continues. Stabilization could occur by changes in rise duration, rise slope, plateau duration, and/or relaxation slope. We demonstrate a generally applicable method for quantifying the relative contribution changes in these characteristics make to contraction stabilization. Our data show that all characteristics change as contractions stabilize, but their relative contribution differs depending on stimulation cycle period and duty cycle. The contribution of changes in rise duration did not depend on period or duty cycle for the 1-, 1.5-, and 2-s period regimes, contributing ~30% in all cases; but for the 0.5-s period regime, changes in rise duration increased from contributing 25% to contributing 50% as duty cycle increased from 0.1 to 0.8. At all cycle periods decreases in rise slope contributed little to stabilization at small duty cycles but increased to contributing ~80% at high duty cycles. The contribution of changes in plateau duration decreased in all cases as duty cycle increased; but this decrease was greater in long cycle period regimes. The contribution of changes in relaxation slope also decreased in all cases as duty cycle increased; but for this characteristic, the decrease was greatest in fast cycle period regimes, and in these regimes at high duty cycles these changes opposed contraction stabilization. Exponential fits to contraction relaxations showed that relaxation time constant increased with total contraction amplitude; this increase presumably underlies the decreased relaxation slope magnitude seen in high duty cycle, fast cycle period regimes. These data show that changes in no single contraction characteristic can account for contraction stabilization in this muscle and suggest that predicting muscle response in other systems in which slow muscles are driven by rapidly varying neuronal inputs may be similarly complex.

## INTRODUCTION

A fundamental goal of neuroscience is to understand the neural basis of behavior. A central component of this goal is to

understand the genesis and control of motor activity. During the last 50 years, tremendous strides have been made, most notably in particularly advantageous, primarily invertebrate, model systems, in describing the neural mechanisms that generate the motoneuron firing patterns that induce movement. During the same period, tremendous strides have also been made in describing muscle excitation:contraction coupling and muscle input:output characteristics. This work has shown that muscles are highly nonlinear and that in general, movement cannot be predicted by linear extrapolation from motoneuron activity. Unfortunately the work on the neural mechanisms that generate motoneuron patterned activity, and the work on muscle contraction characteristics, have generally occurred in different preparations, and hence in no system do we have a complete understanding of the neural genesis of motor behavior. This is even more unfortunate because, since neural networks evolved to create behavior, it is possible that certain aspects of these networks exist to compensate for, or take advantage of, muscle nonlinearities.

We have been attempting to remedy this situation in one of the best understood of all neural networks, the pyloric neural network of the lobster (*Panulirus interruptus*) stomatogastric system, by studying the input:output characteristics of the muscles the network innervates (Ellis et al. 1996; Koehnle et al. 1997; Morris and Hooper 1997, 1998a,b; Morris et al. 2000). This work has shown that these muscles are very slow (relaxation time constants in the 3- to 5-s range). The pyloric network produces a neural output pattern in which the motoneurons fire 100–250 ms bursts every 0.5–2 s, and consequently the pyloric muscle contractions each motoneuron burst induces cannot fully relax during the subsequent interburst interval. The contraction induced by each motoneuron burst therefore “builds” on the relaxation phase of the contraction induced by the preceding motoneuron burst. The response to repeated motoneuron bursts is thus a staircasing in which the contraction each burst induces (the *phasic* component of the contraction) is added to a temporally summated background contraction (the *tonic* component of the contraction) that is a function of system history.

Temporal summation occurs whenever a repetitive input activates a response whose relaxation is slow in comparison with the input’s repeat period. Temporal summation is found not only in a variety of rhythmically driven slow muscles

Address for reprint requests: S. L. Hooper, Neuroscience Program, Dept. of Biological Sciences, Irvine Hall, Ohio University, Athens, OH 45701 (E-mail: Hooper@ohio.edu).

The costs of publication of this article were defrayed in part by the payment of page charges. The article must therefore be hereby marked “advertisement” in accordance with 18 U.S.C. Section 1734 solely to indicate this fact.

(Atwood 1973; Carrier 1989; Ellis et al. 1996; Hall and Lloyd 1990; Hetherington and Lombard 1983; Koehnle et al. 1997; Mason and Kristan 1982; McPherson and Blankenship 1992; Morris and Hooper 1998a; Morris et al. 2000), but also in a variety of neurobiological processes including changes in intracellular calcium concentration and enzyme activity in response to synaptic input (Blinks et al. 1978; De Koninck and Schulman 1998; Hanson et al. 1994; Putney 1998; Rome et al. 1996), summation of postsynaptic potentials in neurons and muscle fibers, and fusion of muscle twitches into tetani.

An important aspect of many temporally summing systems is that system response often reaches stable state at amplitudes less than the maximal (saturated) response of the system—e.g., in response to rhythmic neural activity, at steady state most slow muscles reach maximum contraction amplitudes that are less than the largest contraction the muscle can produce. To achieve steady state at sub-maximal levels, some characteristics of the phasic contractions must change during the rhythm's initial cycles so that the increase in phasic contraction amplitude that each motoneuron burst induces and the decrease in phasic contraction amplitude that occurs during each interburst interval become equal, and thus the temporally summated tonic contraction ceases to change. Prediction of motor output from neural input critically depends on these changes in phasic contraction characteristics, and these changes have seldom been examined in detail.

We have therefore investigated how contraction characteristics change as isotonic contractions of the slow, nontwitch pyloric dorsal dilator muscle of the lobster stabilize in response to rhythmic neural input. Both the amplitude and the temporal characteristics of the phasic contraction change to allow steady state to be attained. We have developed a method to quantitatively compare these changes, and report that at different cycle periods and duty cycles the muscle uses different mechanisms to achieve steady state. A preliminary report of these data has appeared in abstract form (Morris and Hooper 1998b).

#### METHODS

Spiny lobsters (500–1,000 g) were obtained from Don Tomlinson Commercial Fishing (San Diego, CA) and maintained in aquaria with chilled (12°C) circulating artificial seawater. Stomachs were dissected from the animals in the standard manner (Selverston et al. 1976) except that the hypodermal origin of the dorsal dilator (cpv1b) muscle pair was preserved. Care was taken to ensure that digestive juices never contacted the muscles and that the muscles were never stretched. Preparations were continuously superfused with chilled (12–15°C), oxygenated *Panulirus* saline with 40 mM glucose. The data shown here are from four experiments.

The dorsal dilator (cpv1b) muscles are a bilaterally symmetric muscle pair inserting on ossicles XXXI on the medial dorsal surface of the pylorus and originating on the dorsal carapace (Fig. 1). They are innervated by the two pyloric dilator (PD) neurons (Maynard and Dando 1974), which travel to the muscles through the dorsal ventricular (dvn), lateral ventricular (lvn), and dorsal lateral ventricular (dlvn) and/or gastropyloric (gpn) nerves. Contractions were induced by stimulation of the lvn or the pyloric dilator (pdn) nerve (which also contains PD neuron axons) after the dvn was cut to prevent spontaneous pyloric network activity from reaching the muscle. Each experiment lasted between 24 and 36 h. Muscle stability during this time was assessed by occasionally delivering a standard pulse train to the muscle and observing whether the muscle response was the same as at earlier times; in all cases reported here, muscle response properties remained constant throughout the experiment.

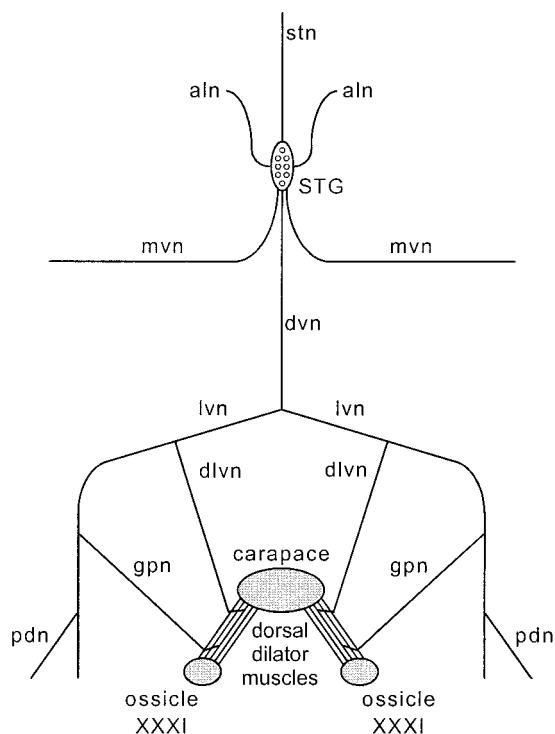


FIG. 1. Experimental preparation. The dorsal dilator muscles insert on ossicles XXXI of the pyloric stomach and originate on the dorsal carapace. They are innervated by the pyloric dilator (PD) neurons of the stomatogastric ganglion (STG). The PD neuron axons travel to the muscles via the dorsal ventricular (dvn), lateral ventricular (lvn), and dorsal lateral ventricular (dlvn) and/or gastropyloric (gpn) nerves and are also present in the pyloric dilator (pdn) nerves. Muscle contractions were induced by stimulation of the lvn or pdn after the dvn had been cut to prevent spontaneous PD neuron activity from reaching the muscle.

All electronics were standard. Nerves were stimulated using polyethylene suction electrodes. Stimulation voltages were increased until maximum muscle contraction amplitudes were achieved, and hence presumably the axons of both PD neurons were being stimulated. Contractions were measured by attaching a Harvard Apparatus 60-3000 isotonic transducer to a wire hooked through the hypodermis between the cpv1b muscle pair. Rest muscle length was maintained at approximately physiological levels. Muscle loading was determined by observing contractions elicited by nerve stimulation with a single burst of shocks using physiologically relevant parameters. We consistently found that loads that produced the largest muscle contractions were often insufficient to return the muscle to its rest length. Muscle load was therefore adjusted to achieve the maximum contraction amplitude consistent with full muscle relaxation subsequent to the stimulation. A support bar was then placed under the end of the transducer arm to prevent muscle overstretching between contraction trains. Transducer output was amplified 20- to 50-fold by a Tektronix AM502 differential amplifier. Contraction characteristics were measured using Spike II (Cambridge Electronics Design) and Kaleidagraph (Synergy Software) after transfer (Cambridge Electronics Design 1401 laboratory interface) to a Gateway 2000 P5. Statistics were performed with Kaleidagraph or SPSS software. Although the full range of stimulation paradigms were attempted with all muscles, in some cases, data from only three of the muscles were usable. We were therefore unable to use paired sample *t*-tests in all cases. In Fig. 6 [comparison of single (1st) and stable contractions], all data were paired, and paired sample *t*-tests were used. Alternatively, in the comparisons between different data points in Fig. 9, the data are not necessarily paired, and for these data, an independent sample *t*-test, with equal variances not assumed, was used. A  $P < 0.05$  significance

level was used throughout. Figure 3 was made using a model developed with Stella II (High Performance Systems) software.

Much of the analysis reported here required linear approximation of the rhythmic and single contraction profiles (Fig. 2). As a first step in this process, we observed the muscle relaxations after the rhythmic stimulations to determine the relaxation dynamics from the contraction amplitude induced by each stimulation paradigm. Figure 2A shows 10 examples of 1.5 s of these relaxations drawn from the data set so as to span the entire contraction amplitude range. In all cases the relaxation phases during this period would be well captured by a linear fit. Since in all our stimulation paradigms intercontraction interval is  $<1.5$  s, we therefore approximated contraction relaxation with a straight line.

The majority of the rise phase is also well fit with a straight line (Fig. 2B). How to define the beginning and end of the broad, relatively flat region at the peak of the contraction (the plateau phase) was more difficult. Trial and error showed that the following procedure (Fig. 2B, *top*) was robust, appeared to well capture the changes in contraction shape that occurred in the various trains, and did not induce gross distortions in contraction amplitude. Lines were drawn to approximate

the rise and relaxation phases of the contractions (solid sloping lines). The slopes of the rise and relaxation lines were determined, and new lines with slopes one-third of these lines were drawn (dashed sloping lines marked "relax 1/3" and "rise 1/3"). These lines were moved to the part of the contraction with a matching slope, and horizontal lines were drawn from the middle of the region of overlap between the contraction and the one third slope lines on both the rise and relaxation sides (horizontal dashed lines marked "relax horiz" and "rise horiz"). A new horizontal line (top solid horizontal line) was drawn and centered vertically between the rise and relaxation horizontal lines. This line and the original rise and relaxation lines were extended to meet, and the length of the resulting horizontal line was identified as plateau duration. A line whose length equaled cycle period was then drawn, and it was moved, and the original rise and relaxation lines extended, until all three lines touched (bottom horizontal line). This linearized contraction was then used to measure rise, plateau, and relaxation durations, rise and relaxation slope, and contraction amplitude.

This procedure had to be modified for contractions induced by a single burst because in these contractions the relaxation phase is not cut short by a subsequent contraction (Fig. 2B, *bottom*), and hence it is unclear where on the relaxation phase to place the original line. For these contractions the rise line, the one-third slope rise line, and the rise horizontal line were all determined as in the preceding text. The intersection of the rise horizontal line and the relaxation phase of the contraction was then identified as the approximate time of the plateau end, and the slope of the contraction between this point and the end of the relaxation duration present in the corresponding rhythmic contractions (vertical lines with arrows) was used to draw the relaxation line in the bottom trace. The one-third relaxation slope and relaxation horizontal lines, and the plateau line, were then determined as usual. Contraction duration was determined by drawing a vertical line at the beginning of the contraction, extending the rise line to meet it, and then extending a horizontal line from this intersection to meet the relaxation line; contraction characteristics were again measured from the resulting trapezoid.

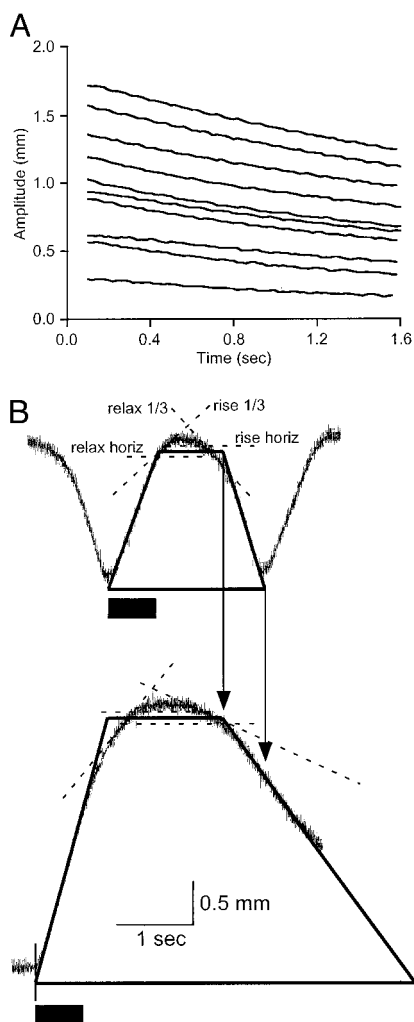


FIG. 2. Linearization of dorsal dilator muscle contractions. A: 1.5 s of relaxation of temporally summated muscle contractions drawn from the data set so as to span entire range of observed contraction amplitudes. In all cases a linear fit would well capture the data. B: explanation of linearization procedure for phasic (*top*) and single (*bottom*) contractions. See text for details. Filled rectangles under traces indicate the durations of the motor neuron bursts used to induce the contractions.

## RESULTS

The *top traces* with rectangles in Fig. 3, A and B, show the motor nerve stimulations that were used to induce the dorsal dilator muscle contractions shown in the graphs below the traces. In Fig. 3A a 2-s cycle period, 60-Hz intraburst spike frequency, 0.25 duty cycle stimulation paradigm was used. Duty cycle ("DC" on figure) equals burst duration ("BD") divided by period ("Per"), and so in this example each rectangle in the upper line represents a 500-ms duration, 31 spike shock burst. In all data reported here, a 60-Hz intraburst spike frequency, which is physiological for the motor neurons that innervate the dorsal dilator muscles, was used. Figure 3B shows the muscle contractions induced by a stimulation paradigm with the same intraburst spike frequency and duty cycle, but a cycle period of 0.5 s.

In each case, the muscle contracts with each burst and relaxes between each burst. However, at the beginning of the stimulation train the muscle relaxes too slowly to fully relax during the interburst intervals present in Fig. 3, A or B. Subsequent contractions therefore "build" on the preceding relaxation phase, and the muscle develops a sustained tonic contraction (dashed lines). The muscle contraction thus consists of phasic contractions and relaxations in time with the bursts of rhythmic nerve stimulation and an underlying tonic contraction.

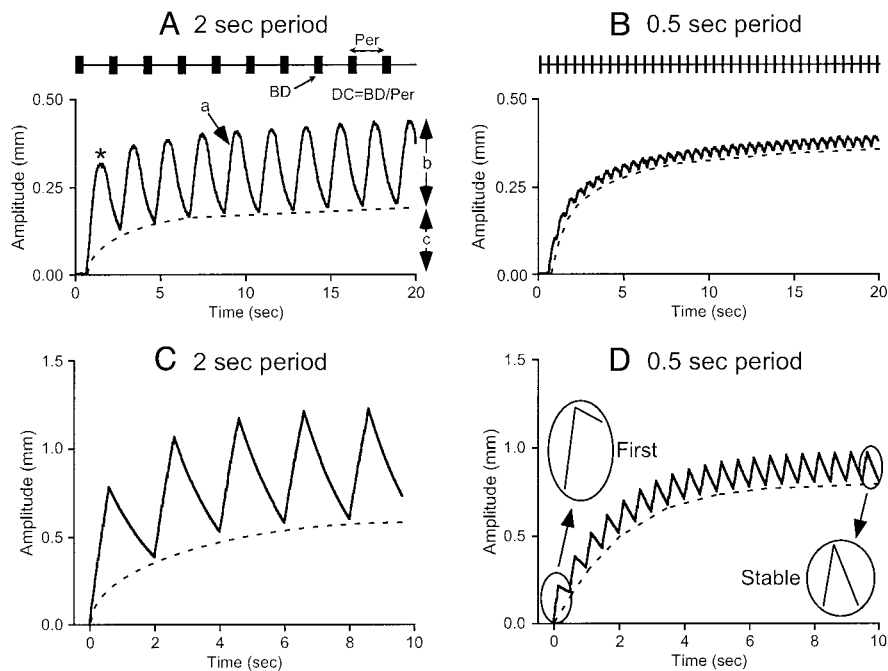


FIG. 3. Comparison of contraction stabilization at 2- and 0.5-s cycle periods and constant duty cycle (0.25) and interburst spike frequency (60 Hz) of the dorsal dilator muscle (A and B) and a simple muscle model (C and D). A and B, top: schematic of nerve stimulation; in A, each rectangle represents a 500-ms, 31-spike shock burst; in B, each rectangle represents a 125-ms, 8-spike shock burst. Arrows, labels, and equation define duty cycle (see text). A: muscle stabilization at a 2-s cycle period. In response to rhythmic nerve stimulation, the contractions induced by each burst temporally summate so that the muscle contraction consists of phasic and tonic (dashed line) components. Eventually the tonic component becomes largely unchanging, which we refer to as stabilization. Arrows, labels, and asterisk on contraction trace define various terms used to describe temporally summated contractions; see text. B: muscle stabilization at a 0.5-s cycle period. In response to rhythmic nerve stimulation, the contractions induced by each burst temporally summate so that the muscle contraction consists of phasic and tonic (dashed line) components. Eventually the tonic component becomes largely unchanging, which we refer to as stabilization. Arrows, labels, and asterisk on contraction trace define various terms used to describe temporally summated contractions; see text. C: model muscle contraction at a 2-s cycle period. D: model muscle contraction at a 0.5-s period. Insets: phasic contraction amplitude decreases, and relaxation slope increases, as the tonic component of the contraction stabilizes. In C and D, all model parameters are constant; contraction stabilization occurs solely as a result of the increased relaxation slope that occurs as contraction amplitude increases.

The presence of two components in summated muscle contractions can potentially lead to confusion when referring to various aspects of the contraction. Throughout this article contraction amplitude refers to the muscle's present contraction amplitude; for instance, at the point at  $\sim 9$  s marked "a" on the contraction curve in Fig. 3A, the muscle's contraction amplitude is  $\sim 0.4$  mm. Tonic amplitude refers to the total amplitude of the tonic component (double headed arrow on Fig. 3A marked "c"). Phasic contraction amplitude refers to the total amplitude of the phasic component alone (double headed arrow on Fig. 3A marked "b"); when the amplitudes of the rise and relaxation of the phasic component differ (e.g., the first phasic contraction of the train, asterisk), the terms phasic rise amplitude and phasic relaxation amplitude are used. In this article we are concerned with changes in the characteristics of the phasic contractions, and throughout, all references to contraction characteristics (rise, plateau, and relaxation duration; rise and relaxation slope, see METHODS and Fig. 2) refer to the phasic contractions. A final convention that is used throughout concerns relaxation slope. Relaxation slope is a negative number. When relaxation becomes more rapid, this slope becomes more negative, and hence, although the absolute magnitude of the slope increases, the slope itself, strictly speaking, decreases. However, in our experience stating that relaxation slope is decreasing inevitably leads to the mistaken perception that relaxation is slowing instead of accelerating. Therefore throughout this article when relaxation becomes more rapid (relaxation slope becomes more negative), we state that relaxation slope increases.

As is apparent in Fig. 3B, the tonic amplitude increases rapidly early in the train and then increases only very slowly. If the train is continued, this late slow increase also ceases, but this can take as long as 1–2 min, which, given the number of conditions tested, was too long a stimulation time to use in these experiments. Control experiments showed that in all stimulation paradigms the tonic component achieved 95% of

its final amplitude within the first 10 s of the stimulation. We therefore defined tonic amplitude as having reached steady state after 10 s of stimulation (although steady-state measurements were always taken well after this time; generally 25–30 s after the beginning of the train), and we refer to the process by which tonic amplitude ceases changing as stabilization.

The purpose of the work reported here was to investigate the mechanisms underlying tonic amplitude stabilization. One possible mechanism is simply that the muscle is reaching the maximum contraction it can produce. However, in Fig. 3, A and B, the muscle stabilized at amplitudes well below the amplitude ( $\sim 1.75$  mm) that would be achieved with a 60-Hz tetanic stimulation; this suggests that other mechanisms underlie the tonic stabilization process.

Insight into these mechanisms can be gained by considering the results of a very simple model of a slow muscle. In this model, each motor neuron spike induces a constant, 0.03 mm, increase in muscle contraction amplitude, and the muscle relaxes toward zero with a single exponential that is sufficiently slow (relaxation time constant 5 s) that at the beginning of the stimulation the contractions cannot fully relax during the subsequent interburst intervals. Figure 3C shows the output of the model muscle in response to a slow cycle period stimulation paradigm (2-s cycle period, 0.3 duty cycle, 60-Hz intraburst spike frequency), and is thus comparable to Fig. 3A; Fig. 3D shows the output in response to a fast cycle period stimulation paradigm (0.5-s cycle period, 0.3 duty cycle, 60-Hz intraburst spike frequency) and is thus comparable to Fig. 3B. In each case tonic amplitude stabilized 5–6 s after the train began, and in each case the stable-state contraction amplitude was well below the amplitude ( $\sim 2$  mm) that would be achieved with a 60-Hz tetanic stimulation.

The model contractions stabilize because the model muscle's relaxation is exponential, and thus as contraction amplitude increases, relaxation slope increases. [During the relaxation phase, contraction amplitude (*Amp*) equals the

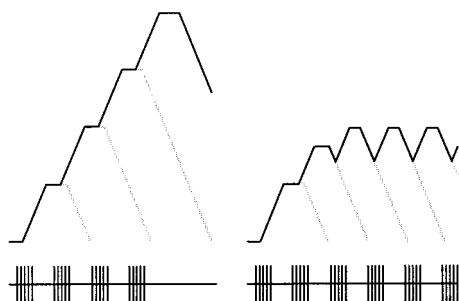


FIG. 4. In multi-component contractions, contraction stabilization need not occur as a result of relaxation slope increases. *Left*: temporal summation if no phasic contraction component changes. Contraction amplitude continually increases and would continue to do so until the maximum contraction the muscle could produce was achieved (not shown). *Right*: as the train continues, phasic rise and plateau duration progressively decrease while keeping rise and relaxation slope constant. The changes in rise and plateau duration both decrease phasic contraction amplitude and increase relaxation duration, and hence the contraction can stabilize at an amplitude less than the maximum the muscle can produce.

amplitude at the beginning of the relaxation ( $Amp_0$ ) times the exponential decline, or

$$Amp = Amp_0 \cdot e^{-t/\tau}$$

and so

$$\frac{dAmp}{dt} = -\frac{Amp_0}{\tau} e^{-t/\tau}$$

and so as contraction amplitude increases so does relaxation slope.] This increase in relaxation slope has two effects (Fig. 3D, insets). First, as contraction amplitude increases the rise amplitude of the phasic contraction induced by each motor-neuron burst decreases [compare rise amplitudes of the first (*left inset*) and final (*right inset*) contractions] because, although each motor-neuron spike induces the same increase in muscle contraction, the relaxation amplitude between each spike in the burst increases as contraction amplitude increases. Second, it increases the amplitude of the relaxation that occurs between bursts [compare relaxation amplitudes of the first (*left inset*) and final (*right inset*) contractions]. Eventually phasic rise amplitude decreases sufficiently, and phasic relaxation amplitude increases sufficiently, to become equal, at which point tonic contraction amplitude stabilizes.

The model thus suggests that in the muscle tonic amplitude stabilizes because phasic relaxation slope increases as contraction amplitude increases. However, close comparison of the muscle and model reveals that at least one aspect of the stabilization process in the two cases differs. In the model, the relative decrease in phasic contraction amplitude that occurs as tonic amplitude stabilizes is the same in both stimulation paradigms (in Fig. 3, C and D, phasic contraction amplitude decreases by 23% from the 1st to the final contraction). However, in the muscle, the relative change in phasic contraction amplitude between the first phasic contraction and those where tonic amplitude is stable differs considerably in the two cycle period stimulations. In the 2-s cycle period stimulation (Fig. 3A), phasic contraction amplitude decreases  $\sim 23\%$ , whereas in the 0.5-s cycle period stimulation (Fig. 3B), phasic contraction amplitude decreases  $\sim 70\%$ .

These data suggested that dorsal dilator tonic amplitude stabilization might not be a simple function of relaxation slope

increasing as contraction amplitude increases with phasic contraction temporal summation. In a system with multiple characteristics such as that shown in Fig. 2B, many different mechanisms can result in tonic amplitude stabilization. Figure 4 shows one such mechanism. The *left panel* shows the muscle's response if no characteristic of the phasic contractions changed; the phasic contractions would continually temporally summate until the muscle achieved its maximum contraction amplitude (not shown). The *right panel* shows the muscle response if phasic contraction rise and plateau duration decreased without changing rise or relaxation slope. Decreasing rise and plateau duration increases relaxation duration. The increased relaxation duration increases phasic relaxation amplitude (since phasic relaxation amplitude equals relaxation duration times relaxation slope). Decreasing rise duration also decreases phasic rise amplitude (since phasic rise amplitude equals rise duration times rise slope). The decrease in phasic rise amplitude and increase in phasic relaxation amplitude eventually result in phasic rise and relaxation amplitudes equalizing, and tonic amplitude therefore stabilizes.

The possibility that changes in phasic contraction characteristics other than relaxation slope are involved in tonic amplitude stabilization was supported by experiments in which contractions were induced by constant cycle period stimulation with a variety of duty cycles (Fig. 5; cycle period, 2 s; the filled rectangles underneath the plot are schematic representations of the stimulation pattern used in the rhythmic muscle stimulations). These data show that tonic contraction amplitude at stable state increases as duty cycle increases. If tonic amplitude stabilization was due to relaxation slope increasing with tonic

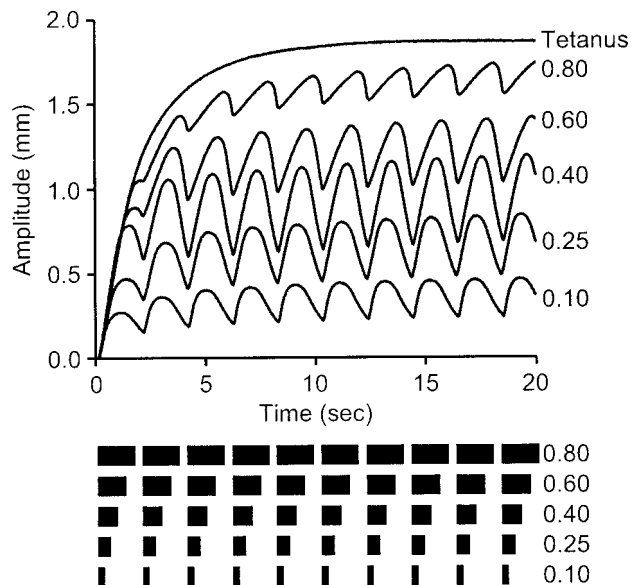


FIG. 5. Dorsal dilator muscle stabilization different duty cycles does not appear to depend solely on an increase in relaxation slope. Despite large increases in contraction amplitude as duty cycle increases from 0.4 to 0.8, relaxation slope increases only slightly. Similarly, in those conditions in which the comparison is possible (the 0.1, 0.25, and 0.4 duty cycle trains), relaxation slope does not appear to markedly increase within a train as it progresses (compare the relaxation phases of the first, second, and third phasic contractions in each train). Numbers on *right* of plot indicate the duty cycle of the various trains. All trains had a 2-s cycle period. The filled rectangles under the plot are schematic representations of the stimulation pattern used in the rhythmic muscle stimulations. Burst duration equals duty cycle times 2 s; intraburst spike frequency was 60 Hz in all stimulation paradigms.

amplitude, the relaxation slope of the higher duty cycle contractions should be greater than those of the lower duty cycle contractions. However, comparison of the stable contractions in the 0.4, 0.6, and 0.8 duty cycle stimulations shows that, despite the large increase in tonic amplitude, very little, if any, increase in relaxation slope occurs as duty cycle and tonic contraction amplitude increases. Similarly, if an increase in relaxation slope was responsible for stabilization, one would also expect to see, in each individual stimulation train, a progressive increase in relaxation slope as the train progressed. This comparison is difficult, particularly in the high duty cycle trains, because the relaxation phase of the early phasic contractions is cut off by the next contraction in the train. However, comparison of the relaxation phases of the first, second, and third (at which point stabilization is largely complete) contractions in the 0.1, 0.25, and 0.4 duty cycle trains shows no apparent increase in relaxation slope.

Although these data suggest that changes in phasic contraction characteristics other than an increase in relaxation slope are involved in tonic amplitude stabilization, observation of rhythmic trains alone cannot be used to address the question of

what changes occur as a train progresses because, particularly at more rapid cycle periods, the relaxation and plateau phases of the early contractions are cut off by the next contraction in the train (see, for instance, Fig. 3B and the 0.6 and 0.8 duty cycle stimulations in Fig. 5). We therefore modified our stimulation protocol so that we also delivered a single burst of shocks with parameters that matched the bursts given in the rhythmic stimulation trains (single contractions). These contractions should be identical to the first contractions in a train, but since they are not followed by subsequent contractions, their plateau durations and relaxation slopes can be measured. We then linearized the single contractions, and the rhythmic contractions at stable state (METHODS, Fig. 2B) and used these data to compare the rise, plateau, and relaxation durations; rise and relaxation slopes; and phasic contraction amplitudes of the first (single) and stable state contractions.

Figure 6 shows summary data for rise duration (row 1), plateau duration (row 2), relaxation duration (row 3), phasic amplitude (row 4), rise slope (row 5), and relaxation slope (row 6) for single (1st) contractions (●) and stabilized contractions (○) for 0.1, 0.2, 0.3, 0.4, 0.6, and 0.8 duty cycles at cycle

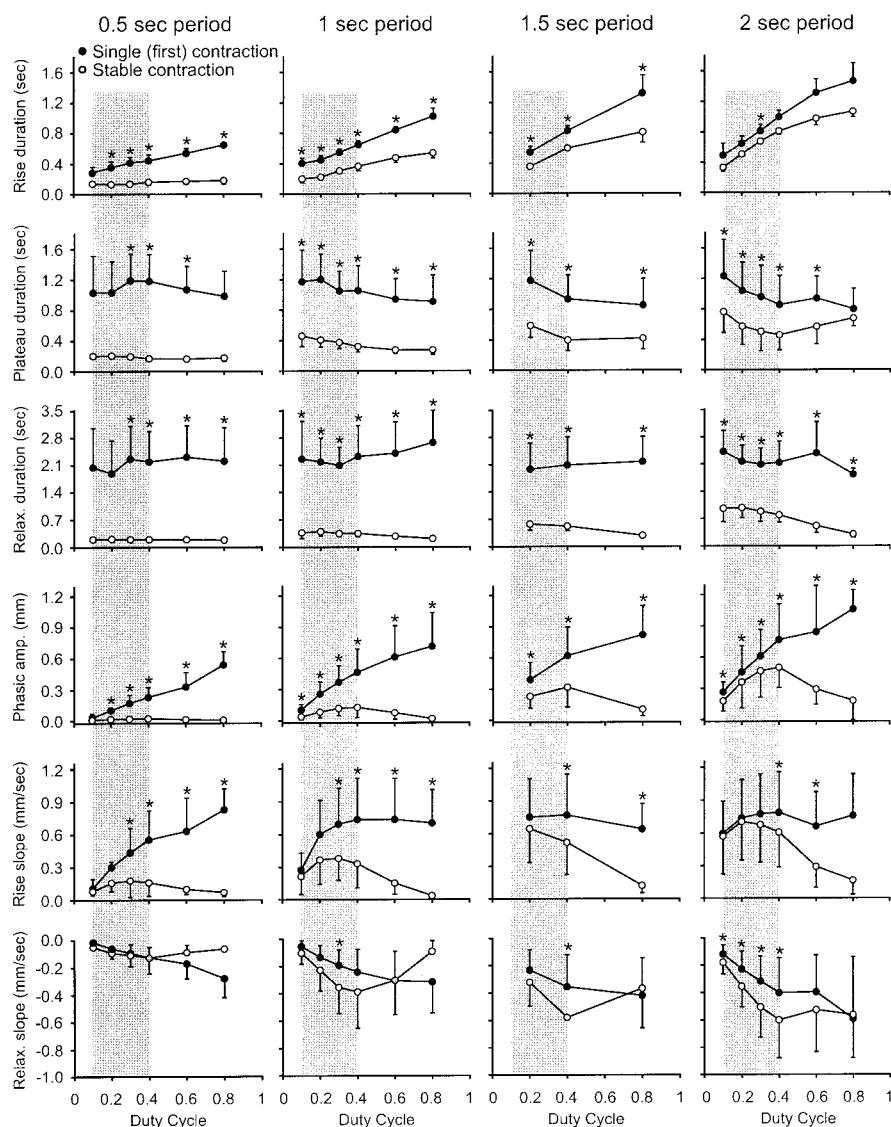



FIG. 6. Variation in phasic contraction components as tonic contraction amplitude stabilizes. Rise duration, plateau duration, relaxation duration, phasic amplitude, and rise slope (rows 1–5) all decrease as tonic amplitude stabilizes, although the magnitude of these decreases is cycle period and duty cycle dependent. Relaxation slope (row 6) increases—becomes more negative—at low duty cycles but remains unchanged or even decreases (which would oppose contraction stabilization) at higher duty cycles. Shading represents physiological duty cycle range. \*, cases in which stable and single (1st) contractions were significantly different. For single contractions, a single shock burst with a burst length matching that applied in the various rhythmic conditions was applied to the motor nerve (for example, in the 1-s cycle period, 0.4 duty cycle case, the single contraction was elicited with a 400-ms duration shock burst). All stimulations were with a 60-Hz intraburst spike frequency.

periods of 0.5, 1, and 2 s and for 0.2, 0.4, and 0.8 duty cycles at a 1.5-s cycle period (all stimulations had a 60-Hz intraburst spike frequency). These cycle periods span the physiological range, and in each plot,  shows the physiological duty cycle range of the input this muscle receives (J. B. Thuma, L. G. Morris, and S. L. Hooper, unpublished data); muscle response across the entire duty cycle range was measured to obtain a general understanding of the muscle's response profile.

Rise duration decreases (which would promote tonic contraction stabilization) between the first and the stable contraction at all cycle periods and duty cycles. These decreases are significant (\*) for almost all data points in the 0.5-, 1-, and 1.5-s period regimes but are significant in the 2-s regime only for the 0.3 duty cycle stimulation. Plateau duration decreases (which would promote tonic contraction stabilization) between the first and stable contraction at all cycle periods and duty cycles. However, the magnitude of this decrease decreases as cycle period increases. In the 2-s cycle period regime, the decrease in plateau duration also decreases with duty cycle, and in the 0.8 duty cycle case, the decrease is no longer significant. Relaxation duration decreases (which would promote tonic contraction stabilization) between the first and stable contractions at all cycle periods and duty cycles, and there is no apparent dependence of this decrease on cycle period or duty cycle. Phasic amplitude decreases (which would promote tonic contraction stabilization) between the first and stable contractions at all cycle periods and duty cycles, and in each cycle period regime this decrease increases with duty cycle. Rise slope decreases (which would promote tonic contraction stabilization) between the first and stable contractions at all cycle periods and duty cycles, and at all cycle periods this decrease increases with duty cycle. Relaxation slope changes relatively little, and these changes are seldom significant except in the 2-s cycle period regime. At all cycle periods at low duty cycles relaxation slope increases (becomes more negative) between the first and stable contractions; this would promote tonic contraction stabilization. However, this decrease decreases as duty cycle increases, and at all cycle periods at high duty cycles relaxation slope is less (more positive) than the single (first) contraction; this would oppose contraction stabilization.

Taken together, these data suggest that in different cycle period and duty cycle regimes, changes in rise duration, plateau duration, relaxation duration, phasic amplitude, rise slope, and relaxation slope may have different relative importance in tonic contraction stabilization. For instance, the change in plateau duration is large in the 0.5-s cycle period condition at all duty cycles but continuously decreases as duty cycle increases in the 2-s cycle period condition. Similarly, changes in relaxation slope in the 0.2, 0.3, and 0.4 duty cycles in the 2-s cycle period regime are much larger than the changes at these duty cycles in the 0.5-s cycle period regime. However, as we show later, determining relative importance of changes in these characteristics is not straightforward and cannot be determined by simple comparison among these data. [As an aside, also note the striking nonproportionality of rise duration on motorneuron burst length. In the 0.5-, 1-, and 2-s cycle period cases, as duty cycle increases from 0.1 to 0.8, burst length increases eight-fold, but in no case does rise duration increase more than 3.4-fold (2-s cycle period plot, stable contraction line), and for the stable contraction line in the 0.5-s period regime, the increase in rise duration over the 0.1 to 0.8 duty cycle range is only 1.25-fold. Although not directly relevant to the issue of tonic amplitude stabilization, this observation does highlight the nonlinearity of the input:output relationship in this muscle and the need for detailed, quantitative analysis to relate neural activity to behavioral output.]

The data presented in Fig. 6 summarize the quantitative changes that occur in all phasic contraction characteristics as tonic amplitude stabilizes, but this presentation does not provide an intuitive sense for the changes in the phasic contractions that occur as stabilization proceeds in the different stimulation regimes. We therefore used these values to construct average phasic contraction profiles (Fig. 7) for the 0.2, 0.4, and 0.8 duty cycle cases at all cycle periods for both single (1st) contractions (the large amplitude, long duration contractions in the plots) and phasic contractions when tonic amplitude had stabilized (the small amplitude, short-duration contractions in the plots). The rectangles under each plot are schematic representations of the stimulation pattern used in that plot; the first rectangle is black to emphasize that the single (1st) contractions were induced with a single stimulus burst. Note that, as

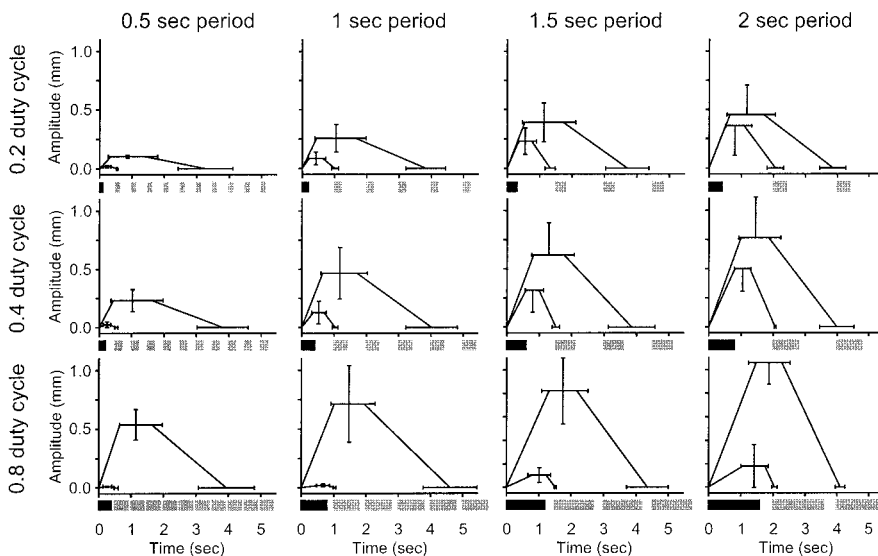


FIG. 7. Averaged profiles of the 1st and stable phasic contractions at 0.2, 0.4, and 0.8 duty cycle (rows) and 0.5-, 1-, 1.5-, and 2-s periods. Again, different mechanisms appear to be more important in different stimulation regimes. For instance, in the 0.2 duty cycle regime, rise slope changes relatively little, whereas in the 0.8 duty cycle regime rise slope changes are large. Rectangles under plots are schematics indicating the burst duration and cycle period of the stimulation used to produce the muscle contractions; the 1st rectangle is filled to emphasize that the first contractions (the large, long duration contractions) were induced with a single burst stimulus.

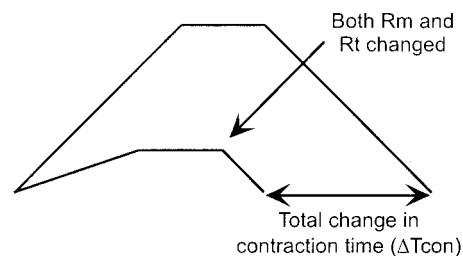
required for tonic contraction stabilization, in all cases the total contraction duration of the phasic contractions equaled stimulation cycle period. These data again suggest that the relative importance for stabilization of changes in the various phasic contraction characteristics vary under different stimulation conditions. For instance, in the 0.2 duty cycle regime (*top*), decreases in rise slope appear to play a relatively small role in contraction stabilization, whereas in the 0.8 duty cycle regime (*bottom*), decreases in rise slope appear to play a major role. Similarly, at low duty cycles relaxation slope increases as the trains stabilize, whereas at 0.8 duty cycle relaxation slope either remains constant (long cycle periods) or even decreases (short cycle periods).

Although these plots provide a qualitative understanding of the changes that cause tonic amplitude stabilization, neither they nor Fig. 6 quantify the relative importance that changes in each characteristic contribute to stabilization. That is, they do not show that, for instance, in the 0.8 duty cycle, 0.5-s cycle period stimulation changes in plateau duration are responsible for 25% of stabilization, whereas in the 0.8 duty cycle, 2-s cycle period changes in plateau duration are responsible for only 5% of stabilization. How to perform this quantification is complicated. Contraction duration ( $T_{con}$ ) equals rise duration ( $R_t$ ) plus plateau duration ( $P_t$ ) plus relaxation duration ( $R_{elt}$ ).  $R_{elt}$  equals contraction phasic amplitude divided by the negative of the relaxation slope ( $Relm$ ; the negative is required because  $Relm$  is negative), and phasic amplitude equals rise slope ( $R_m$ ) times  $R_t$ . Putting these together gives  $T_{con} = R_t + P_t - R_t * R_m / Relm$ . Tonic contraction amplitude stabilizes because as the stimulation train proceeds  $R_t$ ,  $P_t$ ,  $R_m$ , and  $Relm$  change so that  $T_{con}$  becomes equal to cycle period (since temporal summation between phasic contractions ceases when  $T_{con}$  equals cycle period). Thus one's initial approach to quantifying the relative importance in the tonic contraction stabilization process of changes in  $R_t$ ,  $P_t$ ,  $R_m$ , and  $Relm$  would be to change only one of these terms, calculate the associated change in  $T_{con}$  with the preceding equation, and compare this change to the total change in  $T_{con}$  that occurs in the real stabilization process. However, the presence of the multiplication and division terms involving  $R_t$ ,  $R_m$ , and  $Relm$  in the expression for  $T_{con}$  means that one obtains different answers for their relative importance depending on how the calculation is performed.

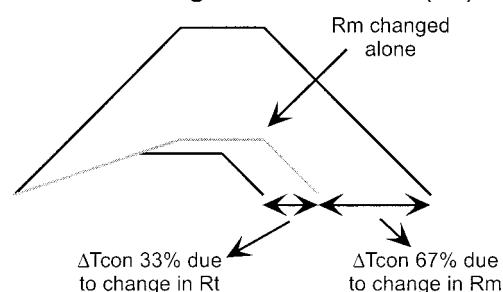
To make this difficulty clear, consider a theoretical example in which changes in only  $R_t$  and  $R_m$  are responsible for tonic contraction stabilization (Fig. 8A). The first contraction (large, long profile) has a 1-s  $R_t$ , 1-mm/s  $R_m$ , 0.5-s  $P_t$ , and  $-1$ -mm/s  $Relm$ ; use of the preceding relations shows that this contraction has a 1-s  $R_{elt}$ , 1-mm phasic amplitude, and 2.5-s  $T_{con}$ . The stable contraction (small, short profile) has a 0.75-s  $R_t$  and 0.33-mm/s  $R_m$ .  $P_t$  and  $Relm$  are the same as in the first contraction, and so the stable contraction has a 0.25-s  $R_{elt}$ , 0.25-mm phasic amplitude, and 1.5-s  $T_{con}$ .

In this example, obviously only changes in  $R_t$  and  $R_m$  contribute to tonic stabilization, but what is the relative importance of the changes in each? Fig. 8B shows the result if we first change  $R_m$  (which results in the gray profile) and then change  $R_t$ . In this case, changing  $R_m$  results in a 667-ms change in total contraction duration. The change in total contraction duration between the initial and stable contractions in Fig. 8A is 1 s. Hence by this analysis, the change in  $R_m$  is 67% responsible for changing the initial contraction into the stable contraction, and thus the change in  $R_t$  is responsible for the

### A Change rise slope ( $R_m$ ) and rise duration ( $R_t$ ) simultaneously



### B First change rise slope ( $R_m$ ) then change rise duration ( $R_t$ )



### C First change rise duration ( $R_t$ ) then change rise slope ( $R_m$ )

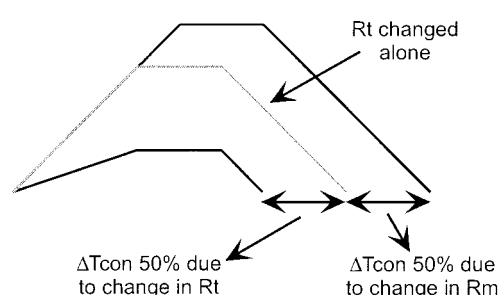


FIG. 8. Relative importance to tonic amplitude stabilization of changes in phasic contraction components depends on the order in which changes in the phasic contraction components are made. A: initial (large, long contraction) and stable (small, short contraction) phasic contraction profiles. The change between the initial and the stable contractions are solely due to changes in rise slope ( $R_m$ ) and rise duration ( $R_t$ ). B: if first  $R_m$  is changed (which results in gray contraction profile), the change in total contraction duration so induced is 67% of the change in total contraction duration between the initial and stable contraction, and hence when analyzed in this manner, the change in  $R_m$  is 67% responsible, and the change in  $R_t$  33% responsible, for stabilization. C: if first  $R_t$  is changed (which results in gray contraction profile), the change in total contraction duration so induced is 50% of the change in total contraction duration between the initial and stable contraction, and hence when analyzed in this manner, the change in  $R_t$  and  $R_m$  are each 50% responsible for stabilization.

remaining 33%. Figure 8C shows the result if we first change  $R_t$  (which results in the gray profile) and then change  $R_m$ . In this case, changing  $R_t$  results in a 500-ms change in total contraction duration, and hence by this analysis, the changes in  $R_t$  and in  $R_m$  are each 50% responsible for changing the initial contraction into the stable contraction.

Which of these analyses is correct? In fact, depending on the physical reality of the stabilization process, both are. If tonic amplitude stabilizes because  $R_m$  first decreases to 0.33 mm/s

while  $Rt$  remains constant, and only after this process is complete, does  $Rt$  decrease to 0.75 s, then the analysis shown in Fig. 8B is correct. Alternatively, if stabilization occurs because first  $Rt$  decreases to 0.75 s while  $Rm$  remains constant, and only then does  $Rm$  decrease to 0.33 mm/s, then the analysis shown in Fig. 8C is correct. As such, the relative importance that changes in phasic contraction characteristics have in tonic amplitude stabilization depends on the temporal evolution of these characteristics relative to each other as the stabilization process proceeds.

This is not a problem specific to temporally summing muscle contractions but will occur in any system in which independent variables interact nonlinearly in determining a dependent variable and is thus one that arises frequently in biological and other systems. If the temporal evolution of the independent variables is known, calculus can be used to resolve this problem unambiguously by integrating along the path the independent variables follow from their initial to final state. In brief, this procedure consists of the following steps.

First, differentiate the equation  $y = f(x_1, x_2, x_3, \dots)$  that defines the relationship between the dependent variable  $y$  and the independent variables  $x_i$  to obtain  $dy = f'_1(x_1, x_2, x_3, \dots) \times dx_1 + f'_2(x_1, x_2, x_3, \dots)dx_2 + f'_3(x_1, x_2, x_3, \dots)dx_3 + \dots$

Second, note that the contribution to  $dy$  made by each independent variable  $x_i$  is

$$dy_{x_1} = f'_1(x_1, x_2, x_3 \dots)dx_1$$

$$dy_{x_2} = f'_2(x_1, x_2, x_3 \dots)dx_2$$

$$dy_{x_3} = f'_3(x_1, x_2, x_3 \dots)dx_3$$

Third, use the experimentally determined temporal evolution equations,  $dx_2 = g_2(x_1)dx_1$ ,  $dx_3 = g_3(x_1)dx_1 \dots$  to express the

equations in the second step in terms of only one of independent variables (in this case,  $x_1$ ).

Fourth, integrate the equations derived in the third step between  $x_{1F}$  and  $x_{10}$  and divide by the total change in  $y$  to calculate the relative contribution that the change in each independent variable makes to the total change in  $y$ .

We provide a detailed explanation (both for a simple illustrative case and for the data presented here) of this procedure in the APPENDIX.

As noted earlier, tonic contraction amplitude stabilization depends only on changes in rise slope, rise duration, plateau duration, and relaxation slope (since phasic amplitude and relaxation time are derived consequences of these characteristics). We performed the analysis outlined above on these four characteristics to determine their relative importance in tonic contraction stabilization as a function of cycle period and duty cycle (Fig. 9). The \* indicate whether the point in question was different from zero ( $P < 0.05$ ); \* that are part of line segments connecting different points indicate whether the two points were different from each other ( $P < 0.05$ ). For instance, in the 0.5-s panel for rise duration (row 1), the points at duty cycles of 0.2, 0.3, 0.4, 0.6, and 0.8 differ from zero and the 0.1 and 0.8 duty cycle points differ from each other.

For 1-, 1.5-, and 2-s cycle periods, the change in rise duration (row 1) made an approximately constant relative contribution of  $\sim 35\%$  to tonic amplitude stabilization. However, in the 0.5-s cycle period regime, the contribution of change in rise duration appeared to be duty cycle dependent, rising from a low of 25% contribution at 0.1 duty cycle to a high of 50% at 0.8 duty cycle.

Change in plateau duration (row 2) made an approximately constant relative contribution of  $\sim 25\%$  in the 0.5-s cycle

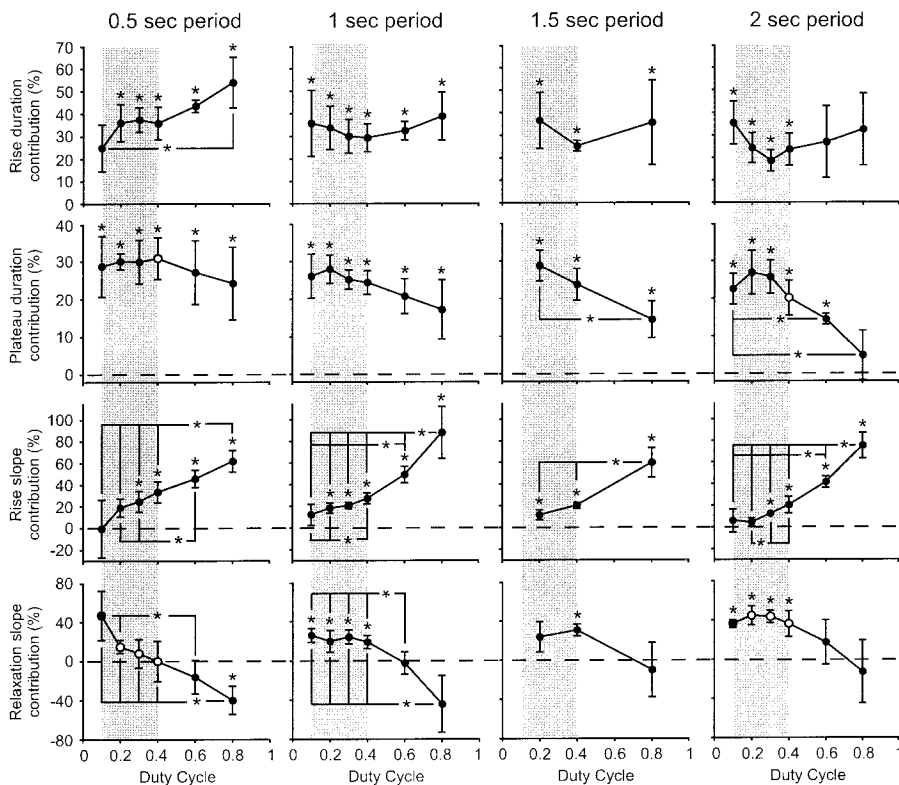


FIG. 9. Relative contribution of changes in rise and plateau duration and rise and relaxation slope to tonic amplitude stabilization at different duty cycles and cycle periods. For rise and plateau duration and relaxation slope, it appears that the contributions of changes in each contraction component depend in many cases on both duty cycle and cycle period. The contribution of changes in rise slope, alternatively, appear to depend only on duty cycle. See text for details. Shading represents physiological duty cycle range.

period regime. As cycle period increased, a negative duty cycle dependence (relative contribution declined as duty cycle increased) of the contribution of change in plateau duration became increasingly apparent. This dependence reached significance in the 1.5- and 2-s cycle period regimes with the relative contribution of change in plateau duration decreasing from 30 to 15% in the 1.5-s cycle period regime, and from 25 to 5% in the 2-s cycle period regime, as duty cycle increased from 0.1 to 0.8. Although this dependence was sufficient to be significant within the 1.5- and 2-s cycle period regimes, it was not large enough to separate equal duty cycles in different cycle period regimes except in the 0.3 duty cycle case in the 0.5- and 2-s cycle period regimes (open data points on plots; the  $P$  value comparing the 0.6 duty cycle cases in the 0.5- and 2-s period regimes was 0.054, the  $P$  value comparing the 0.8 duty cycle cases in the 0.5- and 2-s period regimes was 0.052).

In all cycle period regimes, the relative contribution of change in rise slope (*row 3*) to tonic contraction amplitude stabilization was strongly positively dependent on duty cycle (relative contribution increased as duty cycle increased), rising from contributions of near 0% at a duty cycle of 0.1 to contributions ranging from 60 to 90% at a duty cycle of 0.8. No dependence on cycle period was apparent when equal duty cycle points in different cycle period regimes were compared.

In all cycle periods, the relative contribution of change in relaxation slope (*row 4*) to tonic contraction amplitude stabilization declined as duty cycle increased, decreasing from contributions ranging from 50% (0.5-s cycle period) to 20% (1-, 1.5-s cycle periods) at a duty cycle of 0.1 to 0% (1.5-, 2-s cycle periods) to -40% (0.5-, 1-s cycle periods) at a duty cycle of 0.8, although only in the 0.5- and 1-s cycle period regimes was this decrease significant. Thus, in keeping with the data presented in Figs. 6 and 7, at high duty cycles in the short cycle period regimes the change in relaxation slope actually opposed tonic contraction amplitude stabilization. The suggestion that the decline in contribution with duty cycle is stronger at shorter cycle periods is supported by comparison of the 0.1, 0.2, and 0.3 duty cycle cases between the 0.5- and 2-s cycle regimes (○). At each of these duty cycles, the contribution of change in relaxation slope was significantly less in the 0.5-s cycle period regime than in the 2-s cycle period regime. Thus, the decline in contribution was not only larger but also occurred at lower duty cycles in the 0.5- than in the 2-s cycle period regime.

The decline in the contribution of relaxation slope as duty cycle increased and cycle period decreased is particularly interesting because under these conditions average muscle contraction amplitude increased (Figs. 3, A and B, and 5), and hence relaxation slope should increase for an exponential process with an unchanging time constant. Alternatively, if the time constant of the exponential increased with contraction amplitude, then the amplitude-induced increase in relaxation slope would lessen, or even reverse (as is seen in the short cycle period, high duty cycle conditions in Figs. 6 and 7, in which relaxation slope decreased—became “shallower”—as the contractions stabilized). To determine if this was occurring, for three of our experiments we made exponential fits to the relaxation at the end of every stimulation train. Figure 10 shows the relaxation time constants of these fits as a function of contraction total amplitude (the amplitude at the top of the phasic contractions;  $b$  plus  $c$  in Fig. 3A); relaxation exponential

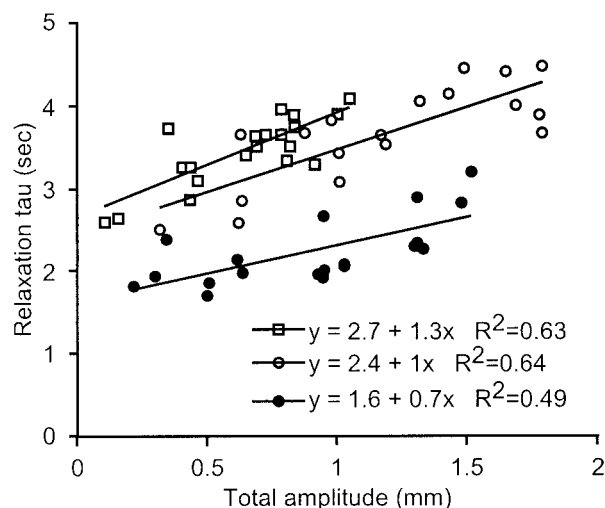


FIG. 10. The dorsal dilator muscle relaxes more slowly as contraction amplitude increases. Exponential fits to the relaxations following the rhythmic stimulations were made in 3 experiments, and the time constants of the exponential were plotted against contraction total amplitude ( $b$  plus  $c$  in Fig. 3). Tau can increase by as much as a second as total contraction amplitude increases from 0.2 to 2 mm.

time constant can increase as much as a second as total contraction amplitude increases from 0.2 to 2 mm.

## DISCUSSION

We have described the changes in the phasic contractions of the dorsal dilator muscle that allow the tonic component of this muscle's temporally summing contractions to stabilize in response to stimulation with rhythmic burst trains. We have also presented a generally applicable method for quantifying the relative importance of each change in this process and shown that the relative importance of each change varies as a function of stimulation cycle period and duty cycle.

### *Generality of the path-dependent relative contribution analysis*

Processes in which one variable depends on the product, power, or similarly nonadditive interaction of two or more other variables are common in biological systems, and we are unaware of a widely used method in biology for apportioning changes in the dependent variable to changes in the independent variables in such cases. The method we describe here is a straightforward application of calculus, its path dependence means that it reflects many of the properties of the system being analyzed, and its ability to express the relative importance of changes in complex systems as single numbers is both a useful, compact description of the system and conceptually satisfying. The use of such integrals is common in engineering and other fields but does not seem to be widespread in biology. These integrals can determine the relative contribution changes in independent variables make to changes of the system as a whole in any biological system in which the temporal evolution of the independent variables can be determined and thus would seem to have widespread utility in biological studies.

### *Implications for the pyloric neuromuscular system*

The pyloric neural network has been intensively studied for almost 25 yr and is one of the best understood of all neural networks (Harris-Warrick et al. 1992). However, because the pylorus is an internal organ and hence not directly observable, almost no data exist as to what motor pattern the network's activity induces. It has often been assumed that the pyloric muscles would be fast enough to accurately follow their neural input and that the motor pattern would thus be a rapid (1 Hz) series of repeated movements (Selverston et al. 1976; Turriano and Heinzel 1992). The data presented here and elsewhere showing that many pyloric muscles are extremely slow, that these muscles respond to pyloric-timed rhythmic input with temporally summated contractions with large tonic components, and that these muscles can express the activity of other, longer cycle period, stomatogastric neural networks that modulate pyloric network neural output (Ellis et al. 1996; Koehnle et al. 1997; Morris and Hooper 1997, 1998a,b; Morris et al. 2000) throw this assumption into question. Unfortunately, due to the internal location and small size of the pylorus, direct measurement of pyloric movements will likely continue to be difficult. An alternative approach is to predict pyloric movement patterns using computer simulation. The data shown here cannot be used directly for this purpose because muscle movement, not tension, was measured. However, the insights into the temporal summation process gained from this work and the analytical techniques developed here should materially advance efforts in developing such models and linking pyloric neural network activity to pyloric behavior.

### *Relevance to fundamental mechanisms underlying muscle response*

The rising phases of the muscle contractions shown here are in response to bursts of action potentials, and as such are a combined response of the muscle to unitary contraction events associated with each neuron spike. The changes in rise slope, rise duration, and plateau duration shown in Figs. 6 and 7 presumably occur as a result of changes in these unitary contractions as a result of stimulation history and the muscle's increased contraction amplitude as the stimulation continues. Unfortunately these unitary contractions are too small to be observed, and it is thus impossible to associate the changes in the characteristics of burst-induced contractions with changes in unitary contraction characteristics.

Nonetheless these data do suggest some tentative conclusions. As was noted in the model contractions shown in Fig. 3, changes in relaxation slope can alter rise slope and amplitude by increasing the amount of relaxation that occurs between each unitary contraction, and it is thus possible that the changes in other contraction components described here could also arise indirectly from changes in relaxation slope alone. However, inspection of Fig. 6 suggests that this is not the case. For instance, in several stimulation regimes relaxation slope does not change as the contractions stabilize (e.g., the low duty cycle cases at 0.5-s cycle period), and yet stabilization still proceeds. Similarly, in several cases relaxation slope decreases, which would, all other things being equal, increase rise slope and phasic amplitude, but in all cases both these components decrease as contractions stabilize. Another mechanism

likely to play a role in decreasing rise slope is the amplitude of the unitary contractions decreasing as the muscle enters the declining portion of its length-tension curve as muscle contraction amplitude increases. However, neither of these mechanisms explains the large decreases in rise duration and plateau duration that are also observed during tonic amplitude stabilization, as it is unclear why decreasing unitary contraction amplitude would decrease unitary contraction rise duration or plateau duration, and the decreases in rise duration and plateau duration appear to be independent of changes in relaxation slope (compare *1st* and *2nd* rows to *bottom* row, Fig. 6). Similarly unexplained is the large increase in relaxation time constant seen as contraction amplitude increases (Fig. 10). Resolution of these issues will require a much deeper understanding of the physical properties of, and excitation-contraction coupling in, this muscle, but at present it appears that tonic amplitude stabilization cannot be explained solely by increasing relaxation slope or decreasing unitary contraction amplitude.

### *Implications for other motor systems*

Considerable evidence from a variety of preparations suggests that temporal summation of muscle contractions could occur in several preparations (Atwood 1973; Carrier 1989; Ellis et al. 1996; Hall and Lloyd 1990; Hetherington and Lombard 1983; Koehnle et al. 1997; Mason and Kristan 1982; McPherson and Blankenship 1992; Morris and Hooper 1998a; Morris et al. 2000; Weiss et al. 1992). Most researchers have implicitly or explicitly considered the tonic contraction associated with temporal summation to be contrary to function (e.g., Weiss et al. 1992), but tonic contraction could be behaviorally beneficial by providing fine motor control by allowing antagonistic muscle co-contraction (Bizzi and Abend 1983), by promoting muscle stiffness and thus allowing muscles to serve as structural elements (Altringham et al. 1993), or by allowing muscles to express the motor patterns of neural networks whose neurons do not innervate them (Morris et al. 2000). In cases in which temporal summation of muscle contractions is behaviorally relevant, prediction of muscle response to varying neural input will critically depend on how phasic contraction characteristics change as a function of muscle contraction history and attained amplitude. Given the exponential nature of muscle relaxation, and the fact that relaxation slope increases with amplitude in exponential processes, it is natural to assume that this increase in relaxation slope would play a, or possibly the, major role in contraction response. However, our data showing that changes in relaxation slope can play a negative (opposing) role in muscle stabilization in certain duty cycle and cycle period regimes and that the relative contributions of other contraction components play large duty cycle and cycle period dependent roles in stabilization, suggest that full understanding of muscle response in such systems may require a detailed analysis of all muscle contraction components. As such, these data underscore the central necessity of a detailed understanding of the neural input to muscle output transfer function for describing the neural genesis of motor behavior.

### APPENDIX

The procedure for determining relative contribution is somewhat involved using the equations that define the phasic contractions (see

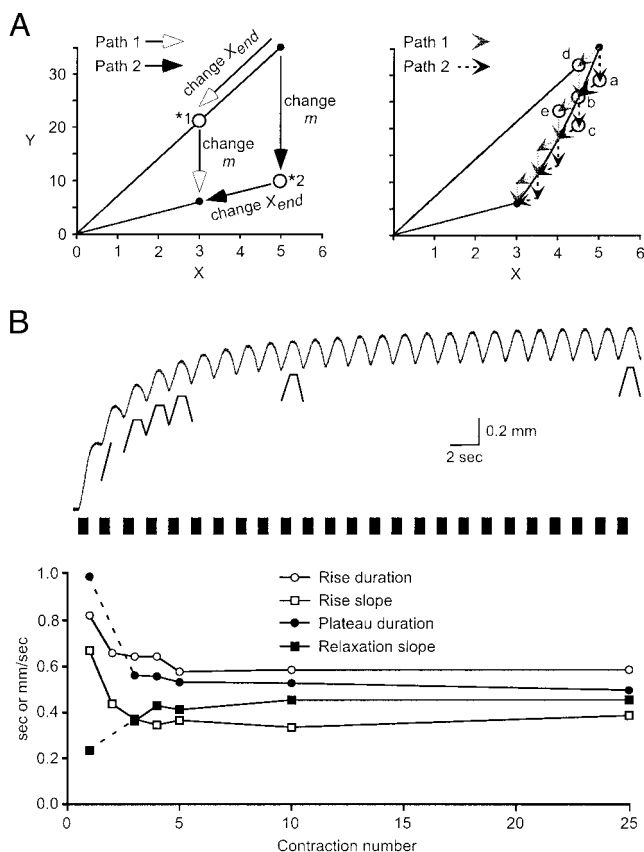


**FIG. A1.** Method to correctly quantify the relative contribution changes in phasic contraction components make to tonic amplitude stabilization. **A:** explanation of quantification method using transformation between 2 line segments as an example. *Right:* 2 paths that connect the top and bottom line segments. *Left:* 2 8-step paths (gray and dashed lines) that connect the segments, and the path if the changes in slope and  $X_{end}$  are proportional and infinitesimal (solid curved line). See text for details. **B:** dorsal dilator muscle contraction characteristics change in synchrony as contraction stabilizes. *Top:* dorsal dilator contraction in response to rhythmic nerve stimulation (*top trace*) and linearizations of 2nd, 3rd, 4th, 5th, 10th, and 25th contractions (line segments under *top trace*). Linearizations have been transposed downward for clarity. Note that for contraction 2 only rise duration and amplitude could be measured. Rectangles are a schematic representation of the stimulation used to generate the muscle contraction. *Bottom:* change in rise duration, plateau duration, rise slope, and the absolute magnitude of the relaxation slope as the train continues. Values for contraction 1 obtained from matching single contraction; dashed lines indicate that plateau duration and relaxation slope could not be measured for contraction 2.

following text), and we have therefore chosen a simpler example with which to demonstrate this analysis initially. Consider transforming one line segment into another (Fig. A1A, *left*). The uppermost line segment runs from (0,0) to (5,35), and therefore has a slope of 7 and an  $X_{end}$  of 5. The bottom line segment runs from (0,0) to (3,6), and therefore has a slope of 2 and an  $X_{end}$  of 3. In the transformation of the first line segment into the second line segment, what is the relative importance of the change in slope versus the change in  $X_{end}$ ? Similar to the case shown in Fig. 8, the answer to this question depends on which path is used to make the transformation. For instance, first changing only  $X_{end}$  from 5 to 3 (path 1) results in arriving at the point marked “\*1” on the plot. This point is (3,21), and the change in  $Y$  due to changing  $X_{end}$  alone is thus  $21 - 35 = -14$ , which is 48% of  $-29$ , the total amount  $Y$  changes in going from line segment 1 to line segment 2. The remaining 52% of the change along this path is due to the subsequent change in slope. Alternatively, first changing only slope from 7 to 2 (path 2) results in arriving at the point marked “\*2” on the plot. This point is (5,10), and along this path, the change in  $Y$

due to changing slope is therefore  $10 - 35 = -25$ . Thus along this path 86% of the total change in  $Y$  is due to the change in slope and only 14% is due to the change in  $X_{end}$ .

Again, each of these values is correct for the different realities they describe; path 1 represents a case in which first  $X_{end}$  and then slope changes; path 2 represents a case in which first slope and then  $X_{end}$  changes. As such, to correctly determine the relative importance of changes in each characteristic, it is again necessary to know how each changes as the others change. Our muscle contractions are fully described by rise duration, rise slope, plateau duration, and relaxation slope (see discussion of Fig. 8), and how these characteristics change with time in a train is therefore the issue at hand. Figure A1B, *top*, shows a 1.5-s cycle period, 0.4 duty cycle rhythmic stimulation, and its corresponding linearizations for the 2nd (only rise duration and slope could be measured for this contraction), 3rd–5th, 10th, and 25th contractions. The rectangles under the trace are a schematic representation of the stimulation used to generate the muscle contraction. Figure A1B, *bottom*, shows the rise durations, rise slopes, plateau durations, and, for ease of presentation, the absolute magnitude of the relaxation slopes of these contractions. Also shown are the values of these contraction characteristics for the corresponding single contraction (the contraction 1 values on the graph). The dashed lines indicate that for contraction 2 plateau duration and relaxation slope could not be measured. It is apparent that all contraction characteristics change in approximate synchrony. This means that the relative change of each characteristic is the same at all times (that is, if rise duration changes by 10% of its total change, rise slope also changes by 10% of its total change).

Knowledge of the path used to go from beginning to final state allows the relative contributions of changes in each characteristic to be unambiguously determined. To demonstrate this procedure, return again to the example shown in Fig. A1A. The data shown in Fig. A1B, *bottom*, indicate that each independent variable is changing in equal proportion of the total change in the variable at all times. Our goal is therefore to go from the original to the final line segment in Fig. A1A by making sequential, constant proportion step changes in line segment slope and  $X_{end}$ . The gray and dashed lines in Fig. A1A, *right*, show the two eight-step paths that result if these two paths are followed by sequentially changing slope and  $X_{end}$  by 1/4 of their total value at each step. The slope of the original line segment is 7, the slope of the final line segment is 2, and thus each slope change will be  $5/4$ ; the  $X_{end}$  of the original line segment is 5, the  $X_{end}$  of the final line segment is 3, and thus each  $X_{end}$  change will be  $2/4$ .

The reason there are two paths is because this procedure can be carried out in two ways—first change slope, then  $X_{end}$ , then slope, then  $X_{end}$ , etc., or first change  $X_{end}$ , then slope, then  $X_{end}$ , then slope, etc. In the dashed path, first slope, then  $X_{end}$ , then slope, then  $X_{end}$ , etc. are changed. The first step (point marked “a” on plot) of the dashed path is thus where the point would be for a slope of  $7 - (5/4) = 5.75$  and an  $X_{end}$  of 5, the second step (point marked “b” on plot) of this path is where the point would be for a slope of 5.75 and an  $X_{end}$  of  $5 - (2/4) = 4.5$ , the third step (point marked “c” on plot) of this path is where point would be for a slope of  $5.75 - (5/4) = 4.5$  and an  $X_{end}$  of 4.5, etc. In the gray path, first  $X_{end}$ , then slope, then  $X_{end}$ , then slope, etc. are changed. The first step (point marked “d” on plot) of the gray path is thus where the point would be for an  $X_{end}$  of  $5 - (2/4) = 4.5$  and a slope of 7, the second step (point marked “b” on plot) of this path is where the point would be for an  $X_{end}$  of 4.5 and a slope of  $7 - (5/4) = 5.75$ , the third step (point marked “e” on plot) of this path is where point would be for an  $X_{end}$  of  $4.5 - (2/4) = 4$  and a slope of 5.75, etc. It appears that the gray and dashed paths are converging on a single path that would be reached were the step sizes infinitely reduced.

This line can be determined as follows. The equation for point  $Y$  is  $y = m * x$ . We are trying to determine the line connecting two such lines as  $m$  and  $x$  change, and we therefore differentiate this

equation to obtain  $dy = x * dm + m * dx$ . Solving this equation for  $x$  requires expressing  $dm$  and  $m$  in terms of  $dx$  and  $x$ . The requirement that  $dm$  and  $dx$  change by the same percentage of their total change means that

$$\frac{dm}{m_F - m_0} = \frac{dx}{x_F - x_0}$$

and so

$$dm = \frac{m_F - m_0}{x_F - x_0} dx$$

Integrating gives

$$m = \left( \frac{m_F - m_0}{x_F - x_0} \right) x + C$$

and recognizing that  $x = x_0$  when  $m = m_0$  allows solving for  $C$ ; the final solution is

$$m = m_0 - \left( \frac{m_F - m_0}{x_F - x_0} \right) x_0 + \left( \frac{m_F - m_0}{x_F - x_0} \right) x$$

Substituting for  $dm$  and  $m$  in  $dy = x * dm + m * dx$  gives

$$dy = \left( \frac{m_F - m_0}{x_F - x_0} \right) x dx + \left[ m_0 - \left( \frac{m_F - m_0}{x_F - x_0} \right) x_0 + \left( \frac{m_F - m_0}{x_F - x_0} \right) x \right] dx$$

which can be solved to give

$$y = \left( \frac{m_F - m_0}{x_F - x_0} \right) x^2 + \left[ m_0 - \left( \frac{m_F - m_0}{x_F - x_0} \right) x_0 \right] x$$

which is the solid curved line in Fig. A1A, *right*. This is the line along which the point at the end of the first line segment would move to reach the point at the end of the second line segment if both  $m$  and  $X_{\text{end}}$  were proportionally, synchronously, and infinitesimally changing.

The relative importance of the changes in  $m$  and  $x$  can be determined by noting that the first term in the right side of the equation  $dy = x * dm + m * dx$  gives the change in  $dy$  due to the change in  $m$  ( $dy_m$ ), and the second term gives the change in  $dy$  due to change in  $x$  ( $dy_x$ ). Thus integrating these terms separately and dividing by the total change in  $y$  gives the desired values. In the case at hand, the change in  $y$  due to the change in  $m$  is  $dy_m = x * dm$ . Substituting the value for  $dm$  noted in the preceding text gives

$$dy_m = \left( \frac{m_F - m_0}{x_F - x_0} \right) x dx$$

Therefore the total change in  $y$  due to changes in  $m$  ( $\Delta y_m$ ) is given by integrating this equation from  $x_0$  to  $x_F$ , and thus

$$\Delta y_m = \left( \frac{m_F - m_0}{2(x_F - x_0)} \right) (x_F^2 - x_0^2)$$

The percent change in  $y$  due to the change in slope is

$$100 * \frac{\Delta y_m}{\text{total change in } y}$$

or 69% in this example. A corresponding integration of the term  $m * dx$  gives a value of 31% for the percent change in  $y$  due to the change in  $x$ .

Turning now to the data presented here, the percent contributions of changes in rise duration ( $Rt$ ), rise slope ( $Rm$ ), plateau duration ( $Pt$ ), and relaxation slope ( $Relm$ ) can be determined as follows. Figure A2 shows a first contraction (the large, long duration contraction) and a stable contraction (the small, short-duration contraction). Total contraction duration ( $Tcon$ ) equals  $Rt$  plus  $Pt$  plus the relaxation duration.

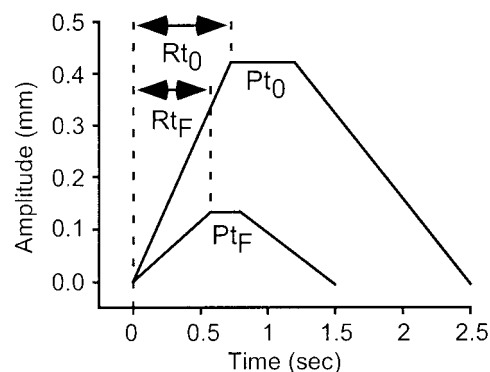


FIG. A2. Quantification of relative contribution changes in each phasic contraction component make to tonic amplitude stabilization. First (the large, long duration) and stable (the small, short-duration) contractions in a train, and rise duration ( $Rt$ ) and plateau duration ( $Pt$ ) are shown; the other relevant contraction components are rise ( $Rm$ ) and relaxation ( $Relm$ ) slope. See text for details.

Relaxation duration equals contraction phasic amplitude divided by the negative of the relaxation slope (the negative is necessary because relaxation slope is negative). Phasic amplitude equals  $Rm * Rt$ , relaxation duration is thus  $Rm * Rt / (-Relm)$  and so  $Tcon = Rt + Pt - Rt * Rm / Relm$ . Differentiating gives

$$dTcon = dRt + dPt - \frac{Rt}{Relm} dRm - \frac{Rm}{Relm} dRt + \frac{Rm * Rt}{Relm^2} dRelm$$

or

$$dTcon = \left( 1 - \frac{Rm}{Relm} \right) dRt + dPt - \frac{Rt}{Relm} dRm + \frac{Rm * Rt}{Relm^2} dRelm$$

The first task is to express each of the variables and the differentials in the right side of this equation in terms of one variable (e.g., to express  $Rm$  and  $Relm$  in terms of  $Rt$  and to express  $dPt$ ,  $dRm$ , and  $dRelm$  in terms of  $dRt$ ), which defines the path along which the subsequent integrations will be made. The fact that all four contraction characteristics change in synchrony means that for any characteristic  $X$

$$dX = \left( \frac{X_f - X_0}{Rt_f - Rt_0} \right) dRt$$

The necessary expressions can therefore be identified as follows.

First, since the term involving  $dPt$  depends on no other characteristics

$$dPt = \left( \frac{Pt_f - Pt_0}{Rt_f - Rt_0} \right) dRt$$

Second, for  $dRm$  and  $Rm$

$$dRm = \left( \frac{Rm_f - Rm_0}{Rt_f - Rt_0} \right) dRt$$

Integrating gives

$$Rm = \left( \frac{Rm_f - Rm_0}{Rt_f - Rt_0} \right) Rt + C$$

and  $C$  can be evaluated by noting that at  $Rm_0$

$$Rm_0 = \left( \frac{Rm_f - Rm_0}{Rt_f - Rt_0} \right) Rt_0 + C$$

Solving gives

$$Rm = \frac{Rm_0 R_{t_f} - Rm_f R_{t_0}}{R_{t_f} - R_{t_0}} + \left( \frac{Rm_f - Rm_0}{R_{t_f} - R_{t_0}} \right) Rt$$

Third, for  $dRelm$  and  $Relm$ , an exactly analogous procedure gives

$$dRelm = \left( \frac{Relm_f - Relm_0}{R_{t_f} - R_{t_0}} \right) dRt$$

and

$$Relm = \frac{Relm_0 R_{t_f} - Relm_f R_{t_0}}{R_{t_f} - R_{t_0}} + \left( \frac{Relm_f - Relm_0}{R_{t_f} - R_{t_0}} \right) Rt$$

The next task is to integrate the  $dRt$ ,  $dPt$ ,  $dRm$ , and  $dRelm$  terms in the  $Tcon$  equation in the preceding text to determine how much of the change in  $Tcon$  is due to changes in each characteristic; the relative change is then determined by dividing these durations by the total change in contraction duration between the first and the stable contraction, and multiplying by 100.

First, the  $dRt$  term is

$$1 - \frac{Rm}{Relm}$$

and the change in contraction duration due to changes in  $Rt$  is thus

$$\Delta Tcon_{Rt} = \int_{R_{t_0}}^{R_{t_f}} \left( 1 - \frac{Rm}{Relm} \right) dRt$$

Substituting the expressions for  $Rm$  and  $Relm$  derived in the preceding text gives

$$\Delta Tcon_{Rt} = \int_{R_{t_0}}^{R_{t_f}} \left( 1 - \frac{Rm_0 R_{t_f} - Rm_f R_{t_0} + (Rm_f - Rm_0) Rt}{Relm_0 R_{t_f} - Relm_f R_{t_0} + (Relm_f - Relm_0) Rt} \right) dRt$$

Identifying  $a = Rm_0 R_{t_f} - Rm_f R_{t_0}$ ,  $b = Rm_f - Rm_0$ ,  $c = Relm_0 R_{t_f} - Relm_f R_{t_0}$ , and  $g = Relm_f - Relm_0$  gives

$$\Delta Tcon_{Rt} = \int_{R_{t_0}}^{R_{t_f}} \left( 1 - \frac{a + bRt}{c + gRt} \right) dRt$$

Direct solution gives

$$\Delta Tcon_{Rt} = \frac{(g - b)(R_{t_f} - R_{t_0})}{g} + \left( \frac{ag - bc}{g^2} \right) \ln \frac{c + gR_{t_f}}{c + gR_{t_0}}$$

Second, the  $dPt$  term is 1, and the change in contraction duration due to changes in  $Pt$  is thus

$$\Delta Tcon_{Pt} = \int_{R_{t_0}}^{R_{t_f}} \left( \frac{Pt_f - Pt_0}{R_{t_f} - R_{t_0}} \right) dRt$$

or

$$\Delta Tcon_{Pt} = Pt_f - Pt_0$$

Third, the  $dRm$  term is

$$- \frac{Rt}{Relm}$$

and the change in contraction duration due to changes in  $Rt$  is thus

$$\Delta Tcon_{Rm} = \int_{R_{t_0}}^{R_{t_f}} - \left( \frac{Rt}{Relm} \right) dRm$$

Substituting the expressions for  $Relm$  and  $dRm$  derived from the preceding text gives

$$\Delta Tcon_{Rm} = \int_{R_{t_0}}^{R_{t_f}} - \left( \frac{(Rm_f - Rm_0) Rt}{Relm_0 R_{t_f} - Relm_f R_{t_0} + (Relm_f - Relm_0) Rt} \right) dRt$$

Substitution of  $b$ ,  $c$ , and  $g$  in the preceding equation gives

$$\Delta Tcon_{Rm} = \int_{R_{t_0}}^{R_{t_f}} - \left( \frac{bRt}{c + gRt} \right) dRt$$

Direct solution gives

$$\Delta Tcon_{Rm} = - \frac{b(R_{t_f} - R_{t_0})}{g} + \left( \frac{bc}{g^2} \right) \ln \frac{c + gR_{t_f}}{c + gR_{t_0}}$$

Fourth, the  $dRelm$  term is

$$\frac{Rm * Rt}{Relm^2}$$

and the change in contraction duration due to changes in  $Rt$  is thus

$$\Delta Tcon_{Relm} = \int_{R_{t_0}}^{R_{t_f}} \left( \frac{Rm * Rt}{Relm^2} \right) dRelm$$

Substituting the expressions for  $Rm$ ,  $Relm$ , and  $dRelm$  derived from the preceding gives

$$\Delta Tcon_{Relm} = \int_{R_{t_0}}^{R_{t_f}} \left( \frac{(Rm_0 R_{t_f} - Rm_f R_{t_0} + Rt(Rm_f - Rm_0))(Relm_f - Relm_0) Rt}{(Relm_0 R_{t_f} - Relm_f R_{t_0} + (Relm_f - Relm_0) Rt)^2} \right) dRt$$

Substitution of  $a$ ,  $b$ ,  $c$ , and  $g$  in the preceding equation gives

$$\Delta Tcon_{Relm} = \int_{R_{t_0}}^{R_{t_f}} g \left( \frac{aRt + bRt^2}{(c + gRt)^2} \right) dRt$$

Direct solution gives

$$\Delta Tcon_{Relm} = \frac{b}{g} (R_{t_f} - R_{t_0}) + \left( \frac{ag - bc}{g^2} \right) \left( \frac{c}{c + gR_{t_f}} - \frac{c}{c + gR_{t_0}} \right) + \left( \frac{ag - 2bc}{g^2} \right) \ln \frac{c + gR_{t_f}}{c + gR_{t_0}}$$

We thank J. S. Connor for useful discussion and advice on the mathematical aspects of the work.

This work was supported by Ohio University, the National Science Foundation, and the National Institute of Mental Health.

## REFERENCES

- ALTRINGHAM JD, WARDLE CS, AND SMITH CI. Myotomal muscle function at different locations in the body of a swimming fish. *J Exp Biol* 182: 191–206, 1993.
- ATWOOD HL. An attempt to account for the diversity of crustacean muscles. *Am Zool* 13: 357–378, 1973.
- BIZZI E AND ABEND W. Posture control and trajectory formation in single- and multi-joint arm movements. *Adv Neurol* 39: 31–45, 1993.
- BLINKS JR, RÜDEL R, AND TAYLOR SF. Calcium transients in isolated amphibian skeletal muscle fibers: detection with aequorin. *J Physiol (Lond)* 277: 291–323, 1978.
- CARRIER DR. Ventilatory action of the hypaxial muscles of the lizard *Iguana iguana*: a function of slow muscle. *J Exp Biol* 143: 435–457, 1989.
- DE KONINCK P AND SCHULMAN H. Sensitivity of CaM kinase II to the frequency of  $Ca^{+2}$  oscillations. *Science* 279: 227–230, 1998.
- ELLIS TA, DONATH AS, MORRIS LG, THUMA JB, AND HOOPER SL. Motor expression of a lateral pyloric constrictor muscle. *Soc Neurosci Abstr* 22: 131, 1996.

- HALL JD AND LLOYD PE. Involvement of pedal peptide in locomotion in *Aplysia*: modulation of foot muscle contractions. *J Neurobiology* 21: 858–868, 1990.
- HANSON PI, MEYER T, STRYER L, AND SCHULMAN H. Dual role of calmodulin in autophosphorylation of multifunctional CaM kinase may underlie decoding of calcium signals. *Neuron* 12: 943–956, 1994.
- HARRIS-WARRICK RM, MARDER E, SELVERSTON AI, AND MOULINS M. *Dynamic Biological Networks. The Stomatogastric Nervous System*. Cambridge, MA: MIT Press, 1992.
- HETHERINGTON RE AND LOMBARD RE. Electromyography of the opercularis muscle of *Rana catesbeiana*: an amphibian tonic muscle. *J Morphol* 175: 17–26, 1983.
- KOEHNLE TJ, MORRIS LG, THUMA JB, AND HOOPER SL. Motor activity of the pyloric and cardiac sac network-innervated cv1 muscle. *Soc Neurosci Abstr* 23: 477, 1997.
- MASON A AND KRISTAN WB JR. Neuronal excitation inhibition and modulation of leech longitudinal muscle. *J Comp Physiol [A]* 146: 527–536, 1982.
- MAYNARD DM AND DANDO MR. The structure of the stomatogastric neuromuscular system in *Callinectes sapidus*, *Homarus americanus*, and *Panulirus argus* (decapoda crustacea). *Philos Trans R Soc Lond B Biol Sci* 268: 161–220, 1974.
- MCPHERSON DR AND BLANKENSHIP JE. Neuronal modulation of foot and body-wall contractions in *Aplysia californica*. *J Neurophysiol* 67: 23–28, 1992.
- MORRIS LG AND HOOPER SL. Muscle response to changing neuronal input in the lobster (*Panulirus interruptus*) stomatogastric system: spike-number versus spike frequency-dependent domains. *J Neurosci* 17: 5956–5971, 1997.
- MORRIS LG AND HOOPER SL. Muscle response to changing neuronal input in the lobster (*Panulirus interruptus*) stomatogastric system: slow muscle properties can transform rhythmic input into tonic output. *J Neurosci* 18: 3433–3442, 1998a.
- MORRIS LG AND HOOPER SL. Predicting pyloric dilator muscle contractions as duty cycle is varied. *Soc Neurosci Abstr* 24: 1891, 1998b.
- MORRIS LG, THUMA JB, AND HOOPER SL. Muscles express motor patterns of noninnervating neural networks by filtering broad-band input. *Nature Neurosci* 3: 245–250, 2000.
- PUTNEY JW JR. Calcium signaling: up down up down . . . what's the point? *Science* 279: 191–192, 1998.
- ROME LC, SYME DA, HOLLINGWORTH S, LINDSTEDT SL, AND BAYLOR SM. The whistle and the rattle: the design of sound producing muscles. *Proc Natl Acad Sci USA* 93: 8095–8100, 1996.
- SELVERSTON AI, RUSSELL DF, MILLER JP, AND KING DG. The stomatogastric nervous system: structure and function of a small neural network. *Prog Neurobiol* 7: 215–290, 1976.
- TURRIGIANO GG AND HEINZEL HG. Behavioral correlates of stomatogastric function. In: *Dynamic Biological Networks: The Stomatogastric Nervous System*, edited by Harris-Warrick RM, Marder E, Selverston AI, and Moulins M. Cambridge, MA: MIT Press, 1992, p. 197–220.
- WEISS KR, BREZINA V, CROPPER EC, HOOPER SL, MILLER MW, PROBST WC, VILIM FS, AND KUPFERMANN I. Peptidergic cotransmission in *Aplysia*: functional implications for rhythmic behaviors. *Experientia* 48: 456–463, 1992.